

## **Silibinin inhibits hepatitis C virus entry into hepatocytes by hindering clathrin-dependent trafficking**

By: Julie Blaising, Pierre L. Lévy, Claire Gondeau, Capucine Phelip, Florence Ruggiero, Stephen J. Polyak, [Nicholas H. Oberlies](#), Tijana Ivanovic, Steve Boulant, Eve-Isabelle Pécheur

**This is the accepted version of the following article:**

Blaising, J., Lévy, P. L., Gondeau, C., Phelip, C., Varbanov, M., Teissier, E., Ruggiero, F., Polyak, S. J., Oberlies, N. H., Ivanovic, T., Boulant, S. and Pécheur, E.-I. (2013), Silibinin inhibits hepatitis C virus entry into hepatocytes by hindering clathrin-dependent trafficking. *Cellular Microbiology*, 15: 1866–1882. doi: 10.1111/cmi.12155,

**which has been published in final form at** <http://dx.doi.org/10.1111/cmi.12155>

### **Abstract:**

Hepatitis C virus (HCV) is a global health concern infecting 170 million people worldwide. Previous studies indicate that the extract from milk thistle known as silymarin and its main component silibinin inhibit HCV infection. Here we investigated the mechanism of anti-HCV action of silymarin-derived compounds at the molecular level. By using live-cell confocal imaging, single particle tracking, transmission electron microscopy and biochemical approaches on HCV-infected human hepatoma cells and primary hepatocytes, we show that silibinin potently inhibits HCV infection and hinders HCV entry by slowing down trafficking through clathrin-coated pits and vesicles. Detailed analyses revealed that silibinin altered the formation of both clathrin-coated pits and vesicles in cells and caused abnormal uptake and trafficking of transferrin, a well-known cargo of the clathrin endocytic pathway. Silibinin also inhibited infection by other viruses that enter cells by clathrin-mediated endocytosis including reovirus, vesicular stomatitis and influenza viruses. Our study demonstrates that silibinin inhibits HCV early steps of infection by affecting endosomal trafficking of virions. It provides new insights into the molecular mechanisms of action of silibinin against HCV entry and also suggests that silibinin is a potential broad-spectrum antiviral therapy

**Keywords:** Hepatitis C virus | milk thistle | silymarin | silibinin | antiviral therapy

### **Article:**

#### **Introduction**

With 170 million individuals infected worldwide, hepatitis C virus (HCV) is a major cause of liver cirrhosis and hepatocellular carcinoma accounting for 40–45% of all liver transplants in the United States (Mukherjee and Sorrell, 2008). Although HCV protease inhibitors were recently approved by the US Food and Drug Administration in combination with interferon-based treatment, these molecules display toxicity and are not effective against all genotypes. A

multidrug regimen targeting various aspects of the viral life cycle will most likely improve HCV therapies. Viral entry is an attractive target for therapeutic intervention, with opportunities to prevent virus binding to receptor(s), internalization and/or fusion. Silymarin, an extract from the seeds of the milk thistle plant *Silybum marianum*, is a popular herbal medicine used as a hepatoprotectant (Tamayo and Diamond, 2007) and inhibits infection by cell culture-grown HCV (Polyak *et al.*, 2007). Its main component, silibinin, is available in a water-insoluble form (called SbN thereafter) and a disuccinate salt injectable form named Legalon-SIL<sup>®</sup>. Clinical trials report that Legalon-SIL<sup>®</sup> but not the insoluble form SbN by oral administration, reduces viral load in patients with chronic hepatitis C (Ferenci *et al.*, 2008; Hawke *et al.*, 2010), even in interferon non-responders (Rutter *et al.*, 2011) and prevents graft reinfection after liver transplantation (Beinhardt *et al.*, 2011). Recent studies reported that high doses of silymarin and silibinin block HCV NS5B polymerase activity *in vitro* (Ahmed-Belkacem *et al.*, 2010; Polyak *et al.*, 2010; Wagoner *et al.*, 2010; 2011). Several reports point to an antiviral activity through inhibition of HCV entry, fusion, transmission and assembly (Wagoner *et al.*, 2010; 2011; Dahari *et al.*, 2011; Polyak *et al.*, 2013). Thus we sought to investigate the mechanisms by which silibinin prevents HCV entry.

Using live-cell imaging studies, we reveal that silibinin inhibits HCV infection of human hepatocytes by blocking its endosomal trafficking. We show that it alters clathrin-mediated endocytosis (CME) and prevents cell infection by viruses that enter through this pathway and require endosomal maturation/triggering. As such silibinin might therefore constitute a potent antiviral compound that targets early stages of the virus life cycle.

## Results

### HCV infects primary human hepatocytes through the clathrin-dependent pathway

At first we characterized how HCV enters human hepatocytes. HCV particles grown in cell cultures (HCVcc JFH-1) were added to Huh7.5 cells and allowed to internalize for up to 20 min. Virions were identified using immuno-electron microscopy (Maillard *et al.*, 2011). Representative micrographs at different time post-infection are shown in Fig. 1A: 5 min post virus addition, virions were found at the plasma membrane, mostly at pseudopod-like cytoplasmic extensions. After 5–10 min, viral particles were associated with intracellular membrane invaginations coated with (electron-dense) clathrin, i.e. clathrin-coated pits (CCP). After  $\approx$  10 min, virions were observed inside clathrin-coated structures. After 20 min, most HCV particles were internalized (Fig. 1B, left). In the presence of the human monoclonal neutralizing antibody CBH-5 (Haid *et al.*, 2009), HCV particle internalization was fully inhibited (Fig. 1B, right; Fig. 1C). CME therefore constitutes an entry route for HCV particles, and inhibition of HCV particle internalization by inhibitors of CME in Huh7 cells further confirms these data (not shown and Blanchard *et al.*, 2006; Collier *et al.*, 2009). To test whether CME also constitutes an infection route for HCV in primary human hepatocytes (PHH), we infected PHH with serum-derived HCV of genotype 1b or 3a, in the absence or presence of chlorpromazine (CPZ).

Inhibition of CME led to a 70–80% decrease in serum HCV infectivity toward PHH (Fig. 1D), in a genotype-independent manner. Of note, CPZ did not exhibit cytotoxicity toward Huh7.5 (not shown) nor PHH cells, under our experimental conditions (Fig. 2A). CME therefore constitutes the main entry route leading to productive infection of human hepatocytes by natural HCV.

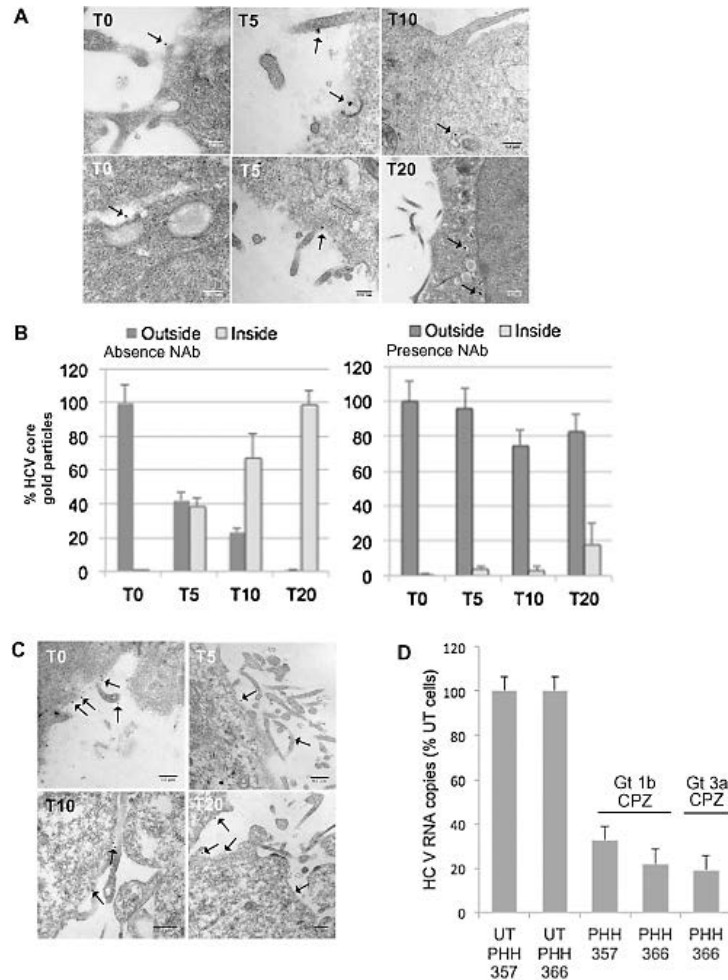


**Figure 1.** HCV enters hepatocytes by clathrin-mediated endocytosis.

A. Huh7.5 cells were incubated with HCVcc JFH-1 (MOI 3) for 30 min at 4°C. Cells were then fixed immediately (T0); or warmed up to 37°C and fixed after 5 (T5), 10 (T10) or 20 min (T20). JFH-1-infected cells were then prepared for immuno-electron microscopy as described (Maillard *et al.*, 2011). HCV was immunolabelled with an anti-E2 AP-33 antibody. Representative micrographs are shown. Arrow, gold-labelled virion.

B. Quantification of JFH-1 internalization: viral particles were added to Huh7.5 cells, in the presence or absence of CBH-5. Virions were immunolabelled for HCV core. For each time point, surfaces of 100  $\mu\text{m}^2$  were analysed and the percent (mean  $\pm$  SD) of non-internalized (dark) or internalized (light) particles among the total number of viral particles was addressed.

C. Representative micrographs obtained in the presence of the CBH-5 antibody; bar, 0.5  $\mu\text{m}$ .

D. Inhibition of serum HCV infection of PHH by CPZ. Three days post seeding, PHH (cultures 357 or 366) were pretreated for 90 min with 20  $\mu\text{g ml}^{-1}$  CPZ and infected with 25  $\mu\text{l}$  serum HCV gt 1b or 3a (viral loads respectively  $2.1 \times 10^7$  and  $7.0 \times 10^6$  RNA copies  $\text{ml}^{-1}$ ). Inoculum was removed after 16 h. Cells were lysed and total RNA was extracted 72 h post-infection. HCV RNA intracellular content was evaluated by RT-qPCR and expressed as percent infection compared with untreated PHH (100%).

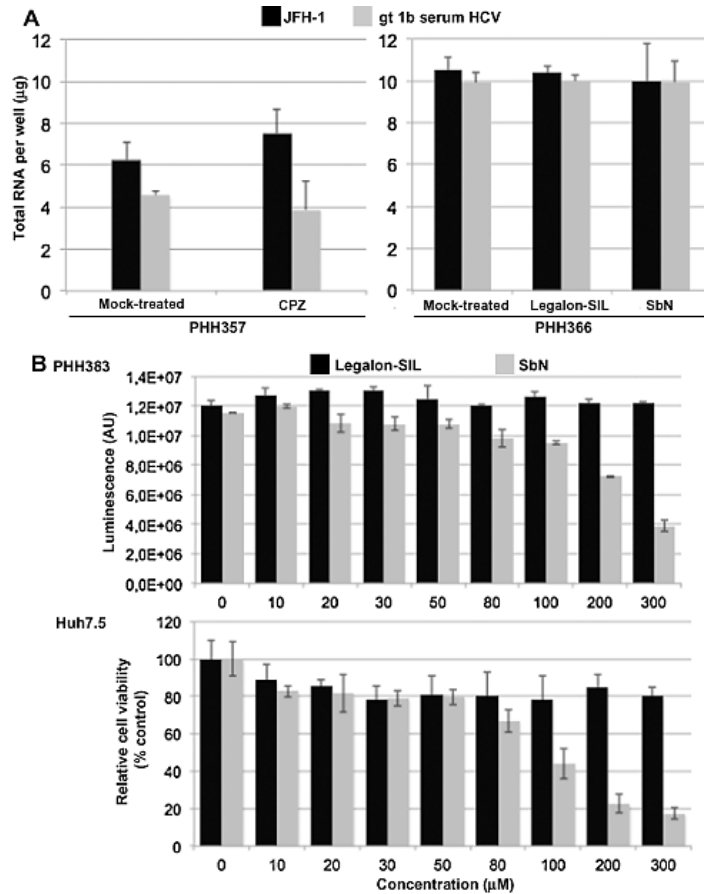


**Figure 2.** CPZ and silibinin are not cytotoxic under experimental conditions.

A. (Left panel) PHH (357) were pretreated with CPZ ( $20 \mu\text{g ml}^{-1}$ , 90 min) and infected with either HCVcc JFH-1 (MOI 1; black) or 25  $\mu\text{l}$  of serum HCV gt 1b (viral load  $2.1 \times 10^7$  RNA copies  $\text{ml}^{-1}$ ; grey). After 16 h at  $37^\circ\text{C}$ , inoculum was removed, monolayers washed with William's E medium and fresh Lanford medium was added. Cells were harvested 72 h post-infection. (Right panel) PHH (366) were mock-treated or treated with 80  $\mu\text{M}$  Legalon-SIL<sup>®</sup> or SbN, incubated at  $37^\circ\text{C}$  for 1h30. Cells were kept 20 min at  $4^\circ\text{C}$ , inoculated with HCV JFH-1 (MOI 1; black) or gt 1b serum HCV (grey) and synchronized 1 h at  $4^\circ\text{C}$ . Cells were then incubated 40 min at  $37^\circ\text{C}$ , inoculi removed and fresh medium containing 80  $\mu\text{M}$  Legalon-SIL<sup>®</sup> or

silibinin was added. PHH cultures were harvested 48 h later for total RNA isolation using a guanidinium isothiocyanate solution (RNAlater, Eurobio), and assayed by Nanodrop™ at 260 nm.

B. Cell viability in the absence or presence of increasing concentrations of Legalon-SIL® or SbN; studies on PHH were performed using the CellTiter-Glo luminescent assay (see *Experimental procedures*). Studies on Huh7.5 cells were based upon the MTS assay and results expressed as percent to control (vehicle alone). Results are means ± SD of triplicate measurements.

### Silibinin is the main inhibitor of HCV fusion in silymarin

We recently showed that silymarin inhibits HCV entry and fusion (Wagoner *et al.*, 2010; 2011). Here, using our HCV/liposome fusion assay (Lavillette *et al.*, 2006; Haid *et al.*, 2009), we identified the flavonolignans from silymarin responsible for the antiviral activity. Among purified compounds, silybin A, isosilybin A and silibinin were the most potent at blocking fusion, followed by silybin B, isosilybin B, silychristin, taxifolin, isosilychristin and silydianin (Table 1). Since silibinin, a 1:1 mixture of silybin A and silybin B, is the major component contained in silymarin, we conclude that most of silymarin's anti-fusion activity is attributable to silibinin. As such, in subsequent experiments we focused on silibinin. We also tested the fusion inhibitory properties of Legalon-SIL®, the water-soluble injectable form of silibinin; this formulation inhibited HCV-mediated fusion in the same micromolar range of concentration as the water-insoluble form of silibinin (termed SbN in the following) (Table 1).

**Table 1. Silibinin is the most potent inhibitor of HCV fusion among silymarin-derived flavonolignans**

Compound	Composition <sup>a</sup> (% total)	HCV fusion inhibition (%)									IC <sub>50</sub> (μM)
		Concentration (μM)									
		10.4	20.7	25	50	75	83	100	125	150	
Silymarin	/	42 ± 2	60 ± 5	66 ± 9	70 ± 3	80 ± 8	84 ± 10	97 ± 2	100	/	15 ± 4
Silibinin	39.8 (16 + 23.8)	22 ± 2	33 ± 4	42 ± 10	66 ± 12	72 ± 6	82 ± 6	83 ± 2	95 ± 3	97 ± 1	34 ± 3
Silybin A	16	10 ± 3	38 ± 6	50 ± 3	58 ± 7	67 ± 9	75 ± 7	81 ± 3	92 ± 3	98 ± 2	25 ± 3

HCV fusion inhibition (%)

Compound	Composition <sup>a</sup> (% total)	Concentration ( $\mu$ M)									IC <sub>50</sub> ( $\mu$ M)
		10.4	20.7	25	50	75	83	100	125	150	
Silybin B	23.8	19 $\pm$ 7	44 $\pm$ 10	48 $\pm$ 6	61 $\pm$ 3	68 $\pm$ 6	70 $\pm$ 8	78 $\pm$ 8	/	100	29 $\pm$ 4
Isosilybin A	6.4	45 $\pm$ 5	58 $\pm$ 10	63 $\pm$ 6	73 $\pm$ 3	/	76 $\pm$ 6	82 $\pm$ 3	94 $\pm$ 4	98 $\pm$ 3	15 $\pm$ 3
Isosilybin B	4.4	39 $\pm$ 7	44 $\pm$ 4	48 $\pm$ 5	56 $\pm$ 8	62 $\pm$ 6	63 $\pm$ 4	70 $\pm$ 5	81 $\pm$ 2	93 $\pm$ 5	31 $\pm$ 4
Silychristin	11.6	19 $\pm$ 6	36 $\pm$ 8	43 $\pm$ 6	49 $\pm$ 4	60 $\pm$ 4	66 $\pm$ 10	73 $\pm$ 6	89 $\pm$ 3	94 $\pm$ 3	53 $\pm$ 3
Isosilychristin	2.2	10 $\pm$ 4	25 $\pm$ 3	/	33 $\pm$ 6	47 $\pm$ 7	51 $\pm$ 8	64 $\pm$ 10	78 $\pm$ 4	87 $\pm$ 5	81 $\pm$ 2
Silydianin	16.7	16 $\pm$ 8	30 $\pm$ 10	/	37 $\pm$ 7	41 $\pm$ 8	48 $\pm$ 9	50 $\pm$ 5	56 $\pm$ 9	73 $\pm$ 6	100 $\pm$ 3
Taxifolin	1.6	28 $\pm$ 8	40 $\pm$ 6	/	48 $\pm$ 8	53 $\pm$ 10	67 $\pm$ 9	71 $\pm$ 8	78 $\pm$ 11	89 $\pm$ 9	60 $\pm$ 3
Legalon-SIL <sup>®</sup>	/	38 $\pm$ 9	43 $\pm$ 3	62 $\pm$ 8	70 $\pm$ 5	78 $\pm$ 7	80 $\pm$ 11	98 $\pm$ 2	100	100	22 $\pm$ 7
DMSO	/	0	0	0	0	0	0	0	2	3	/

<sup>a</sup> Composition of milk thistle products from Madaus GmbH, expressed as % of total material (from Davis-Searles *et al.*, 2005). Note that the total is < 100%, since the remaining 20 to 30% consist of uncharacterized polyphenols and fatty acids. Silibinin consists of silybin A and silybin B in a 1:1 mixture.

Fusion between HCVpp and R<sub>18</sub>-labelled liposomes is measured by recording lipid mixing kinetics by fluorescence spectroscopy (Lavillette *et al.*, 2006). Values of the last 30 s of fusion kinetics (final fusion extent) are used to calculate the percentage of fusion in the absence or

presence of drug. Results expressed as % of fusion inhibition are means± SD of three separate experiments. DMSO, vehicle alone. The IC<sub>50</sub> values for fusion inhibition were calculated.

### Silibinin impedes HCV infection of PHH and endosomal trafficking

Our recent work showed that Legalon-SIL<sup>®</sup> and SbN both inhibit HCVcc infection in Huh7.5 cells (Polyak *et al.*, 2010; Wagoner *et al.*, 2011). Here we show that both formulations inhibit infection of PHH by HCV JFH-1 or serum from HCV-infected patients. Legalon-SIL<sup>®</sup> and SbN treatment of PHH resulted in a 42%- ( $P < 0.05$ ) and 80%-decrease ( $P < 0.005$ ) of JFH-1 infection, respectively, compared with mock-treated cells (Fig. 3A). Similarly, Legalon-SIL<sup>®</sup> and SbN treatment of Huh7.5 cells resulted in a ~ 2-log decrease of HCV JFH-1 infection (Fig. 3B). Serum HCV infection of PHH was also reduced by 76% with Legalon-SIL and 60% with silibinin ( $P < 0.01$ ) (Fig. 3A). Of note Legalon-SIL<sup>®</sup> displayed a greater inhibitory effect on HCV genotype 1b than 2a (JFH-1), which is in line with recent observations that Legalon-SIL<sup>®</sup> inhibits HCV 1b but not 2a subgenomic replicons (Wagoner *et al.*, 2011; Esser-Nobis *et al.*, 2013). Importantly, Legalon-SIL<sup>®</sup> or SbN at the concentration used in this study did not display any cytotoxicity toward PHH nor Huh7.5 cells as measured by quantification of cellular ATP and MTS assay respectively (Fig. 2B).

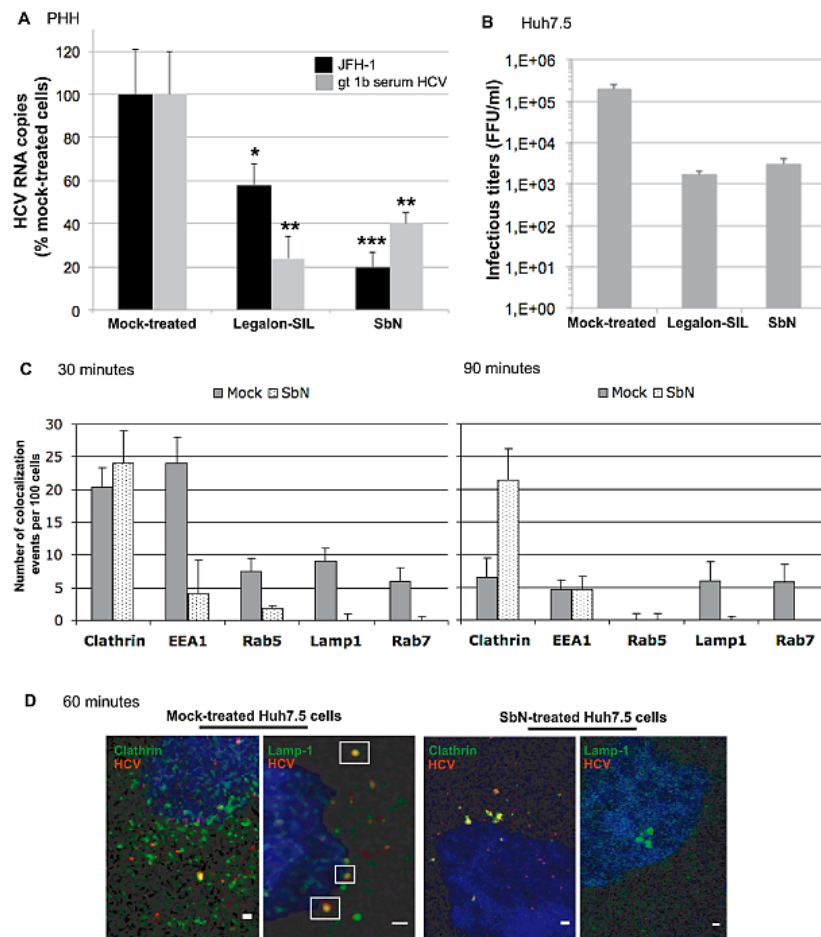


**Figure 3.** Silibinin impedes HCV infection of primary human hepatocytes and endosomal trafficking.

A. PHH were mock-treated with 80  $\mu\text{M}$  Legalon-SIL<sup>®</sup> or SbN, incubated at 37°C for 1h30. Cells were kept 20 min at 4°C, inoculated with HCV JFH-1 (MOI 1; black) or gt 1b serum HCV (grey) and synchronized 1 h at 4°C. PHH were then incubated 40 min at 37°C, inoculi removed and fresh medium containing 80  $\mu\text{M}$  Legalon-SIL<sup>®</sup> or SbN was added. Cells were harvested for total RNA isolation 48 h later. HCV RNA content was expressed as percent infection compared with mock-treated PHH (100%). Results are mean  $\pm$  SD of triplicate measurements.

B. Viral infectivity under 80  $\mu\text{M}$  SbN or Legalon-SIL<sup>®</sup> treatment of Huh7.5 cells was determined by serial dilutions of JFH-1 virions, starting from a MOI of 1. After 72 h in culture, cells were fixed in methanol/acetone, and prepared for immunofluorescence of HCV core using the C7-50 antibody. Fluorescent foci of infection (expressed as FFU  $\text{ml}^{-1}$ ) were then counted under the microscope.

C. Quantification of the number of colocalization events between HCVcc JFH-1 and indicated endosomal markers, counted in 100 cells mock- or SbN-treated; 30 min/90 min, time after transfer of HCV-infected cells to 37°C. Results are mean  $\pm$  SD from two independent experiments (see D).

D. Huh7.5 cells were mock (DMSO)- or pre-treated with 80  $\mu\text{M}$  SbN for 30 min at 37°C, incubated with JFH-1 ( $9.9 \times 10^5$  FFU  $\text{ml}^{-1}$ ; MOI 1) for 1 h at 4°C, in medium containing SbN. After removal of unbound virions, cells in medium containing 80  $\mu\text{M}$  SbN were transferred to 37°C for 60 min, fixed and co-immunostained for HCV core (red) and clathrin light chain or Lamp1 (endo-lysosomal marker) (green).

These data demonstrate that both forms of silibinin are potent inhibitors of serum HCV infection in primary hepatocytes, the most physiologically relevant cell culture model.

To characterize the mechanisms by which silibinin protects human hepatocytes from HCV infection, we used 3D-confocal microscopy to assess HCV intracellular trafficking in Huh7.5 cells. Cells were mock- or pre-treated with SbN, and infected with HCVcc. In the absence of drug, HCV (detected by core red staining) was found associated with clathrin-positive structures and the early endosomal marker EEA1 within 30 min (Fig. 3C). At 60–90 min post-infection, particles separated from the early endosomes and coincided with the late endosomal markers Lamp1 and Rab7 (Fig. 3C and D). In SbN-treated cells, at early and late times post-infection, virions were mostly confined in clathrin-positive structures and a few were found in EEA1-positive structures (Fig. 3C and D). This suggests that SbN impedes HCV intracellular trafficking.

To further study this effect, we followed HCV pseudoparticle (HCVpp) entry and trafficking in Huh7.5 cells using live-cell microscopy. HCVpp were labelled with the lipophilic dye

R<sub>18</sub> (Lavillette *et al.*, 2006), purified and thoroughly characterized. Examination of R<sub>18</sub>-HCVpp by electron microscopy did not reveal any defects (Fig. 4A), and immunofluorescence analyses revealed that the GAG core protein of HCVpp [from mouse leukaemia virus (Bartosch *et al.*, 2003)], HCV E2 and R<sub>18</sub> signals colocalized together in infected cells (Fig. 4B). Quantification performed on 180 cells randomly selected from three separate experiments showed 80% of colocalization between HCV E2 and R<sub>18</sub> signals. HCVpp purified after R<sub>18</sub> incorporation only displayed a 15% loss of infectivity as compared with dye-free HCVpp, indicating that dye incorporation *per se* did not alter HCVpp infectivity.

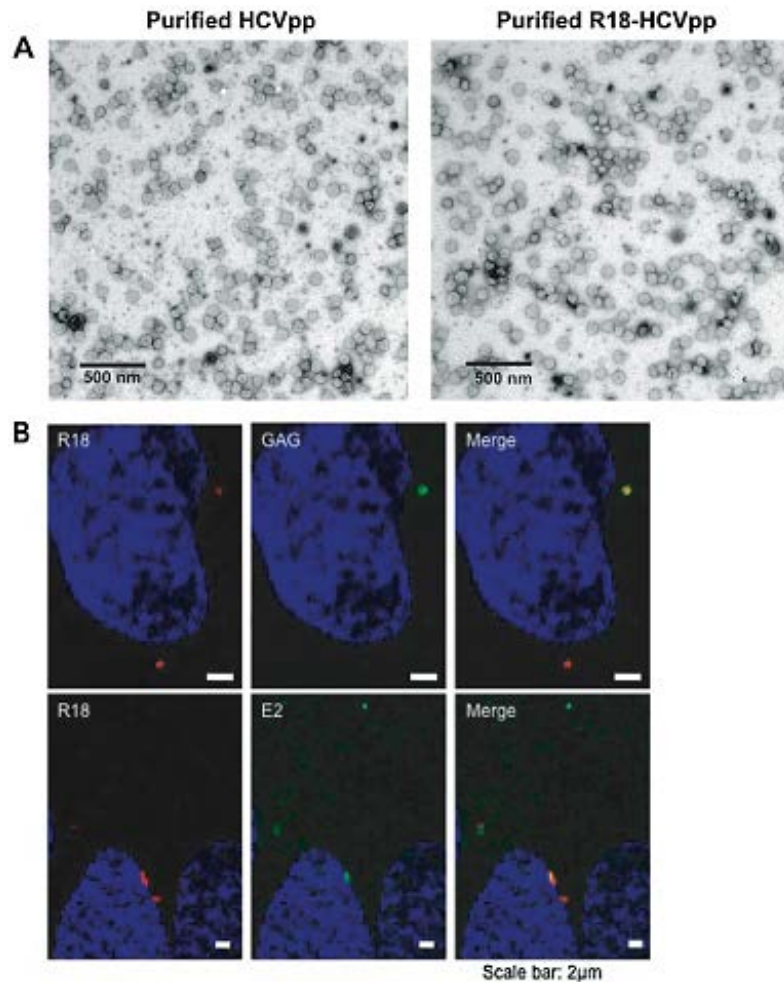


**Figure 4.** Characterization of purified R<sub>18</sub>-HCVpp particles. Pseudotyped particles produced from 293T cells were pelleted through a sucrose cushion and resuspended in either PBS (HCVpp) or PBS containing R<sub>18</sub> (2 nmol per 100 μl particles) (Lavillette *et al.*, 2006) (R<sub>18</sub>-HCVpp), to a final 100-fold concentration compared with cell supernatant. HCVpp, labelled or not with R<sub>18</sub>, were then purified on a sucrose gradient and resuspended in PBS after sucrose removal by centrifugation (see *Experimental procedures*).

A. Electron microscopy (negative staining with uranyl acetate) examination of purified HCVpp, labelled with R<sub>18</sub> or not.

B. Immunostaining of HCVpp with a rat anti-mouse leukaemia virus GAG or a mouse anti-HCV E2 (AP33), followed by secondary goat anti-rat or anti-mouse antibodies coupled to Cy2 or Dylight488 (Pierce) respectively. R<sub>18</sub> fluorescence is directly visualized, and nuclei are labelled with DAPI. Examination is performed using a Zeiss confocal inverted spectral LSM 710.

Huh7.5 cells expressing clathrin light chain fused to enhanced green fluorescent protein (eGFP) were infected with purified R<sub>18</sub>-HCVpp; viruses and clathrin-coated structures were then imaged simultaneously by confocal microscopy (Movie S1). Time-lapse analyses revealed HCVpp association with clathrin-positive structures in Huh7.5 cells. Both clathrin-dependent endocytic events and intracellular trafficking in clathrin-coated structures were visualized. A typical HCV entry event is shown Fig. 5A: during time-lapse acquisition, virions landed at the cell surface. After binding, HCV associated with a discrete eGFP-containing spot (30 s). Clathrin-eGFP signal around the virion then increased, indicating maturation towards a clathrin-coated vesicle (CCV, 30–59 s). Beyond 88 s, clathrin-eGFP signal vanished, presumably due to CCV uncoating (Ehrlich *et al.*, 2004). Following the disappearance of the clathrin signal, a rapid directional movement of the labelled viral particle was observed. This displacement was similar to that observed after clathrin-dependent uptake of other viruses (Ehrlich *et al.*, 2004; Cureton *et al.*, 2009; 2012). On average, clathrin-eGFP signal colocalized with HCV for 30–100 s, consistent with previously observed dynamics of CME events (Ehrlich *et al.*, 2004; van der Schaar *et al.*, 2008).

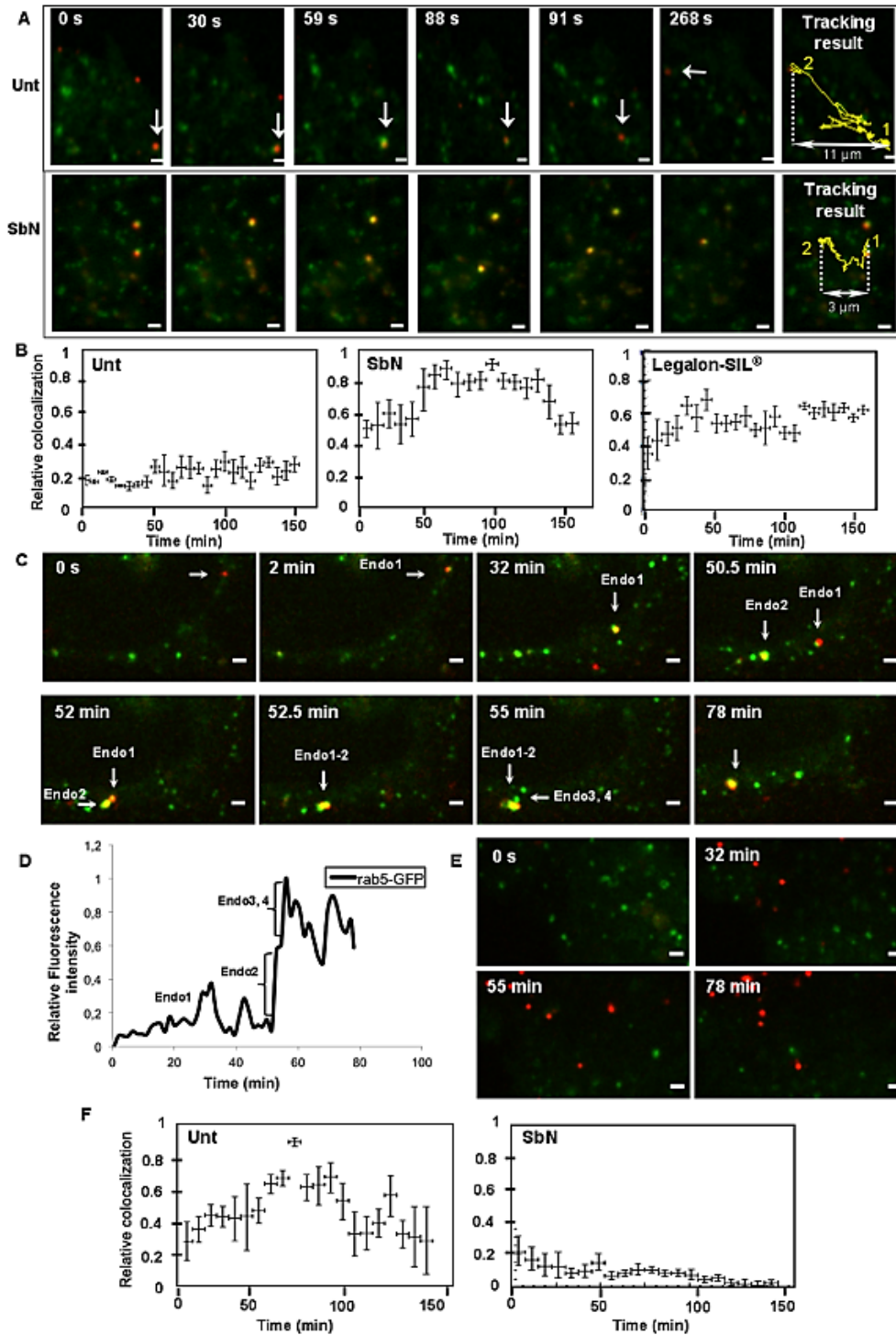


**Figure 5.** Silibinin hinders early entry steps of HCV into Huh7.5 cells.

A. Snapshots of R<sub>18</sub>-labelled HCVpp (red dots, white arrow), internalized in eGFP-clathrin-coated pits (green) in DMSO-treated cells (Unt) (Movie S1) or treated with 80  $\mu$ M SbN (SbN; Movie S2). Yellow trackings indicate beginning (1) and end (2) of HCVpp trajectory. Bar, 1  $\mu$ m.

B. Relative colocalization between clathrin-coated structures and HCV as a function of time, in mock-(Unt), silibinin (SbN)- or Legalon-SIL<sup>®</sup>-treated cells. To estimate the measurement error on the number of colocalization events and HCV, the mean value and standard deviation of these quantities were calculated using counts over a 6 min period (see *Experimental procedures*).

C. Snapshots of R<sub>18</sub>-labelled HCVpp (arrow) trafficking in eGFP-Rab5-positive endosome (Endo1, green) in untreated cell. Endo1 fuses with Endo2 containing HCVpp, followed by fusion with empty Endo3 and Endo4 (Movie S3). Bar, 1  $\mu$ m.

D. Fluorescence intensity profiles of eGFP-Rab5 recruitment to Endo-1 from snapshots in C. Endo-2, -3 and -4 indicate successive fusion with Endo-1.

E. Snapshots of a cell expressing Rab5-eGFP, treated with 80  $\mu$ M SbN and infected with R<sub>18</sub>-labelled HCVpp (red) (Movie S4). Bar, 1  $\mu$ m.

F. Relative colocalization between Rab5-positive structures and HCV as a function of time, in mock-(Unt) or SbN-treated cells.

In SbN-treated cells, HCV remained confined in clathrin-positive structures for a greater period of time. Tracking analyses revealed an overall impediment to movement of HCV- and clathrin-positive structures in SbN-treated vs untreated cells: 3 vs 11  $\mu$ m (Fig. 5A; Movie S2).

We next measured the extent over time of HCVpp colocalization with clathrin-coated structures, in live cells treated or not with SbN/Legalon-SIL<sup>®</sup>. Early post-infection (< 50 min), untreated cells displayed very little colocalization events (Fig. 5B left). Colocalization between clathrin and HCVpp lasted 30–100 s on average, which likely corresponds to endocytic events. At later times post-infection (> 50 min), a greater colocalization level was observed, probably due to HCVpp accumulation in recycling/degradation pathways. Upon treatment with SbN or Legalon-SIL<sup>®</sup> (Fig. 5B middle and right panels respectively), the number of colocalization events increased over time to plateau and was significantly higher than in mock-treated cells. When silibinin is present, HCV virions are then properly internalized but trapped in clathrin-coated structures that accumulate in the cytosol.

We then studied the kinetics of HCVpp trafficking into the early endosomal compartment. R<sub>18</sub>-labelled HCVpp were added to Huh7.5 expressing eGFP-fused Rab5, a GTPase marker of early endosomes. The intracellular location and trafficking of viral particles were addressed by live-cell confocal fluorescent microscopy (Fig. 5C). After internalization, a rapid recruitment of Rab5-eGFP onto virion-containing structures was observed. Fusion events between Rab5-positive endosomes were observed, and virions remained associated for more than 70 min with early endosomes. Kinetic analysis of Rab5-eGFP and HCVpp fluorescence intensities corroborated these observations. During the first 2–3 min, fluorescence rapidly increased due to massive recruitment of Rab5 to the first endosome (Endo1) (Fig. 5D). At 52 min fluorescence drastically increased as Endo1 fused successively with a second endosome also containing

HCVpp (Endo2) and empty endosomes (Fig. 5, Endo3 and 4 and Movie S3). Upon treatment with SbN, no colocalization between HCVpp and Rab5-positive structures was observed (Fig. 5E; Movie S4). This was fully consistent with our observations on fixed samples (Fig. 3C). Statistical analyses indicated a high level of Rab5-HCV colocalization events over time in untreated cells, while it was close to zero in cells treated with SbN (Fig. 5F). These data indicate that in SbN-treated cells, HCV particles remain confined in clathrin-coated structures, and are unable to merge with Rab5-positive early endosomes. Thus silibinin hinders early steps of HCV entry and endosomal trafficking.

### Silibinin hinders entry of other viruses

To determine if silibinin is a general inhibitor of clathrin-dependent virus entry, the effects of SbN on influenza virus infection were tested by measuring *de novo* production of infectious particles. SbN moderately inhibited influenza virus infection of MDCK cells, only when present at pre-entry steps (Fig. 6A, triangles). This inhibition was only partial, since influenza virus also uses clathrin-independent entry pathways (Rust *et al.*, 2004).

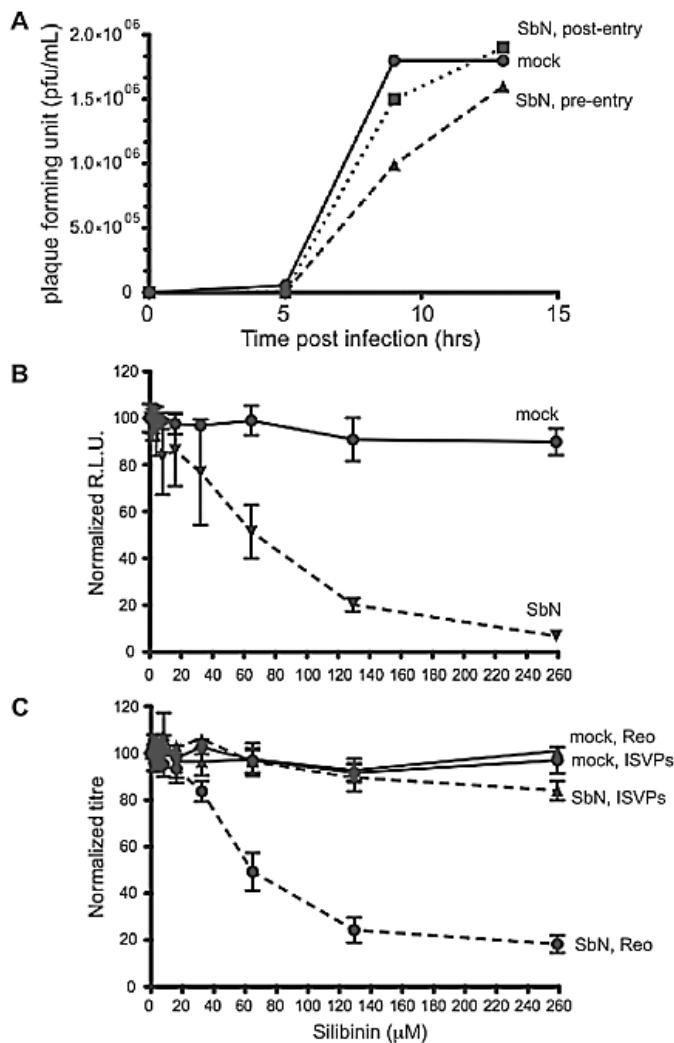


**Figure 6.** Silibinin inhibits infection by viruses that enter cells by CME.

A. MDCK cells were mock- or SbN-treated for 30 min prior to infection. Influenza viruses were added 1 h at 37°C, then washed out. To evaluate SbN effect on post-entry steps, it was added to mock-treated cells 1 h post wash-out. Cells: mock-treated (circles), pre-treated with SbN (pre-entry step, triangles) or treated with SbN after influenza entry (post-entry step, squares).

B. BSC1 cells were mock- or SbN-treated for 15 min. VSV encoding the firefly luciferase gene was added to cells for 30 min. Excess virus was washed with PBS and fresh medium containing SbN was added to infected mock- (solid line) or SbN-treated cells (dashed line). Seven hours later, VSV infection was assayed through firefly luciferase expression, normalized to the signal obtained in untreated cells. Results are mean  $\pm$  SD of a triplicate experiment.

C. Similar as B except that cells were infected 2 h by reovirus virions (circles) or ISVPs (triangles). Two days post-infection, virus production was assessed by plaque assay and results normalized to the titre obtained in untreated cells. Results are mean  $\pm$  SD of a triplicate experiment.

We then evaluated SbN effect on vesicular stomatitis virus (VSV) infection of BSC1 cells (Fig. 6B). An infection assay with a genetically modified VSV encoding firefly luciferase revealed that pretreating cells with SbN prevented infection in a dose-dependent manner. Interestingly the IC<sub>50</sub> of SbN for VSV was similar to that observed for HCV [60 and 40  $\mu$ M (Polyak *et al.*, 2010) respectively], suggesting that the drug might use a similar inhibitory mechanism to block HCV and VSV infection.

We then tested SbN effects on cell infection by the non-enveloped mammalian reovirus. A 70%-reduction in the number of virion-infected cells was observed in the presence of drug (Fig. 6C). Conversely, it did not affect intermediate subvirion particles (ISVPs) infection, which enter cells independently of CME (Martinez *et al.*, 1996). Collectively our results demonstrate that silibinin is a potent inhibitor preventing infection by viruses dependent on the clathrin pathway.

**Silibinin impedes CME in living cells**

Our above results do not address whether observed effects are specific to virus-containing clathrin structures or to any cellular clathrin structure. To address the impact of silibinin on CME, we monitored transferrin (Trf) uptake in Huh7.5 cells (Fig. 7A). Trf is an iron-binding glycoprotein internalized by CME after engagement of its cellular receptor. In untreated cells after a brief internalization, Trf was located at the perinuclear region (Fig. 7A Mock-treated). In SbN-treated cells, Trf was detected in very few cells, either in endosomal compartments located throughout the cell or at the plasma membrane with little or no intracellular localization (Fig. 7A SbN-treated and right panel).

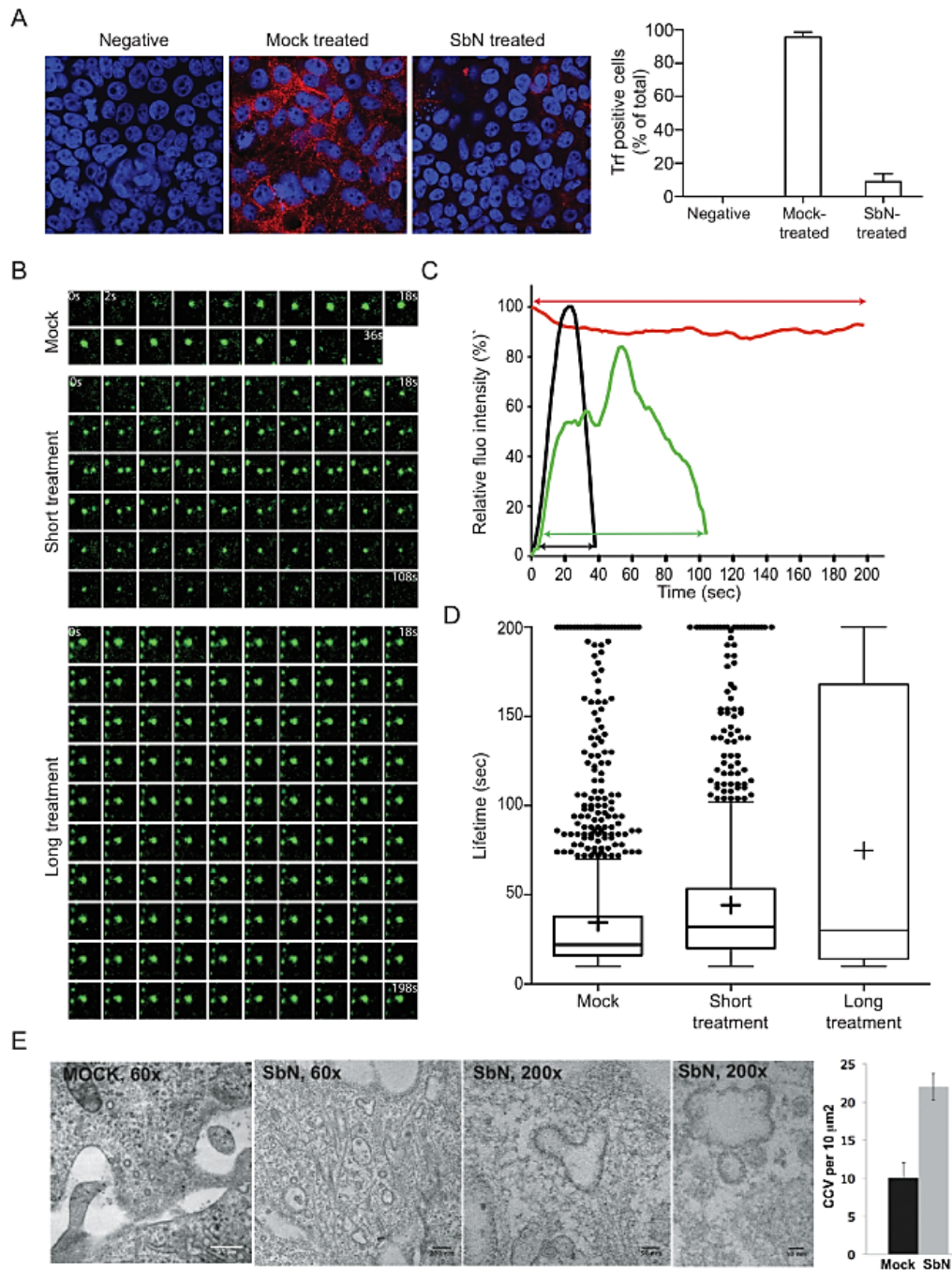


**Figure 7.** Silibinin alters clathrin-mediated endocytosis.

A. Inhibitory effect of silibinin on receptor-mediated uptake of Trf in Huh7.5 cells. Cells were mock- or SbN-treated, incubated with  $50 \mu\text{g ml}^{-1}$  Alexa647 human Trf for 7 min at  $37^\circ\text{C}$  in the absence or presence of SbN, transferred to  $4^\circ\text{C}$ , briefly rinsed with acidic medium to remove membrane-bound Trf and processed for spinning disk confocal fluorescence microscopy. Left, representative images of Trf uptake. Right, histograms depicting the effect of  $80 \mu\text{M}$  SbN on Trf uptake; cell number for each category was normalized to the total number of cells analysed.

B–D. BSC1 cells stably expressing AP-2-eGFP were treated with SbN or DMSO (mock). Dynamics of CCP formation was monitored using spinning disk confocal microscopy, with a 2 s-interval between images (Movies S5, S6 and S7). Short and long treatment: 10 and 25 min respectively.

B. Tile view at 2 s-intervals of representative CCP formation in mock- or SbN-treated cells (short and long treatment).

C. Fluorescence intensity over time of the representative CCP depicted in B, normalized to the maximum fluorescence intensity reached during CCP formation (top of the curve). AP-2-eGFP-labelled pits in mock- (black) or SbN-treated cells (short, green; long, red). The arrows correspond to the lifetime of a CCP, from initiation of the CCP (detection of AP-2-eGFP) to uncoating (disappearance of the AP-2-eGFP signal).

D. Lifetime distribution of CCP forming in mock- or SbN-treated BSC1 cells (short and long treatment). Box and whiskers representation of the CCP lifetime. Data are from at least five cells. Bar in the middle of the box represents the median, the cross represents the average. Upper and lower parts of the box represent upper and lower quartile respectively.

E. TEM examination of Huh7.5 cells treated or not with SbN for 30 min. Left to right: mock- and SbN-treated ( $\times 60$  k); detail of previous ( $\times 200$  k), other detail (id.); quantitative evaluation of CCV per  $10 \mu\text{m}^2$  in mock- or SbN-treated cells ( $P < 0.01$ , Student's *t*-test statistic).

To further characterize silibinin effect on CME, we compared the dynamics of CCP formation in SbN absence or presence. We used our BSC1 cells expressing AP-2-eGFP, prototype cells for clathrin studies (Boulant *et al.*, 2011). Experiments could not be performed in Huh7.5 cells due to instability of the AP-2-eGFP construct in these cells (not shown). The CCP lifespan, corresponding to the elapsed time between appearance and disappearance of AP-2 coat constituents (colour arrows in Fig. 7C) was monitored for mock- and SbN-treated cells. Representative tile views of CCP are represented in Fig. 7B. Statistical analyses revealed that in the absence of SbN, the mean lifespan of CCP structures was  $34 \pm 17$  s (Fig. 7C black; D mock; Movie S5). In contrast, after a 10 min (short) treatment with 50 or 80  $\mu\text{M}$  SbN, the mean lifespan of CCP was significantly longer (Fig. 7C green; D short; Movie S6). After a longer SbN treatment (25 min), CME was progressively impaired and a large part of CCPs were no longer dynamic and arrested at the plasma membrane (Fig. 7C red; D long; Movie S7). About 25% of clathrin-coated structures were stalled in the presence of SbN, as opposed to less than 2% in mock-treated cells. These results demonstrate that silibinin progressively impaired CME by affecting assembly and maturation of clathrin-coated structures.

While the overall cell morphology was not modified by silibinin treatment, ultrastructural changes were observed in the cells. When viewed by transmission electron microscopy (TEM), an abnormal number of enlarged pleiomorphic clathrin-coated structures was observed in SbN-

treated Huh7.5 cells (Fig. 7E). Quantification revealed a 2.2-fold increase in CCV number *per* surface in SbN-treated vs untreated cells ( $P < 0.01$ ).

Altogether these results demonstrate that silibinin impedes CME by affecting either or both assembly and maturation of clathrin-coated structures.

## Discussion

For the first time our study provides molecular details on the mechanism of action of the hepatoprotectant silibinin on hepatitis C virus entry and fusion. Our observations lead to the following conclusions: (i) both silibinin water-insoluble and injectable soluble forms (Legalon-SIL<sup>®</sup>) inhibit HCV infection in human primary hepatocytes; (ii) silibinin hinders HCV endosomal trafficking: viral particles are trapped in clathrin-positive structures and cannot be delivered to the early endosomal compartment, thereby preventing infection; (iii) silibinin globally impedes CME and induces the intracellular accumulation of clathrin-coated structures by a yet unknown mechanism; and (iv) silibinin efficiently hinders infection of cells by several different viruses and as such might constitute a broad spectrum antiviral compound.

Clathrin-mediated endocytosis is the predominant mechanism that cells use to uptake extracellular components. Many viruses have developed strategies to hijack this pathway to gain access to the intracellular environment and infect cells (Mercer *et al.*, 2010). It has been reported that HCV infects cells by the clathrin-dependent pathway (Blanchard *et al.*, 2006; Codran *et al.*, 2006; Coller *et al.*, 2009). Our results confirm these previous observations and demonstrate for the first time that both cell-cultured and serum-derived HCV mostly use CME to productively infect PHH.

Our analyses of HCV entry dynamics at both micro- and nano-metre scales revealed virion internalization into CCP and CCV within the first few minutes of contact between virus and plasma membrane of human hepatoma cells or primary hepatocytes. HCV particle internalization by the clathrin machinery required 30–100 s on average. This agrees well with previous studies, reporting CME of enveloped and non-enveloped viruses achieved within 30–200 s, depending of the viruses (Ehrlich *et al.*, 2004; Rust *et al.*, 2004; Cureton *et al.*, 2009; 2012; Boulant *et al.*, 2013). After internalization of CCP containing virions, CCV uncoat, traffic into the cells and merge with the early endosomal compartments. Our live cell imaging studies of HCV entry revealed numerous fusion events between endocytic vesicles containing HCV and Rab5-positive endosomes, and between Rab5-positive endosomes containing HCV or not. These frequent observations emphasize the role of this GTPase in HCV intracellular traffic (Farquhar *et al.*, 2012). Virions were further sorted through Rab7-positive late endosomes and delivered to endo-lysosomes harbouring Lamp1, most likely for degradation.

Our observations revealed that silibinin alters the very first steps of HCV entry and the subsequent intracellular endosomal trafficking necessary for the acid-dependent triggering of HCV particles. First, rapidly after addition to cells, silibinin significantly reduces the

internalization rate of virions into cells. Second, silibinin altered viral transport from endocytic vesicles to Rab5-positive early endosomes. HCV remained stalled in motionless clathrin-positive structures and no longer colocalized with Rab5-, Rab7- or Lamp1-positive vesicles, indicating a defect on endosomal trafficking. HCV requires access to acidified endosomal compartments to be infectious (Meertens *et al.*, 2006; Tscherne *et al.*, 2006). By impeding intracellular trafficking, silibinin prevents the acid-dependent triggering of HCV, while dropping HCV infectivity. Thus, silibinin anti-HCV activity is likely due to an alteration of intracellular trafficking, leading to a block in viral particle maturation in endosomal compartments.

Reovirus infection requires virion conversion into ISVPs in the endosomal compartment in a pH-dependent manner (Chandran *et al.*, 2002). Conversely direct infection of cells by ISVPs is independent of pH acidification (Martinez *et al.*, 1996). Our results show that only reovirus virion infectivity is decreased in silibinin-treated cells. These findings suggest that silibinin might directly or indirectly affect virion conversion to ISVP, as proper conversion to ISVP in the endosomal compartment would have resulted in efficient infection. As such this observation supports a model where silibinin, by altering endosomal trafficking, would inhibit the pH-dependent triggering of viral particles. This model remains to be carefully demonstrated as the entry route of reovirus ISVPs is unclear and appears to be cell-specific. In some cell types, ISVPs enter by CME while in others they enter either by a caveolin-dependent or in a dynamin-independent pathway (Schulz *et al.*, 2012; Boulant *et al.*, 2013). As such, the lack of inhibition of ISVPs entry by silibinin could be the consequence of ISVPs entering cells in a clathrin-independent manner.

How the effect of silibinin results in a decrease of virion uptake and in an alteration of endosomal trafficking remains unclear. However, we have observed that silibinin induces a slowdown in CCP and CCV rates of formation and TEM analyses revealed accumulation of clathrin-coated structures inside the cytosol. Extended treatment with silibinin induced a nearly complete arrest of CME. This arrest could be due to the depletion of cytosolic free clathrin molecules and coat components, in line with their accumulation onto vesicular structures induced by silibinin treatment. This drop in free clathrin pools could abort or arrest CCP formation at the plasma membrane and indirectly affect intracellular trafficking of endosomal compartments. A similar phenotype has been observed in auxilin-depleted cells. Auxilin is a co-chaperone protein together with heat shock protein cognate 70 (Hsc70), that supports uncoating of CCV. In auxilin-knocked-out primary neuronal cells, CCV number increased and CME was affected. Sequestration of coat components onto CCP and CCV was suggested to be responsible for the arrest of CME (Yim *et al.*, 2010). Silibinin-mediated accumulation of clathrin-coated structures in the cytosol might induce an arrest or slowdown of CME, translating into a reduced internalization rate of HCV.

Alterations of endosomal trafficking could also result from the sequestration of clathrin on cytosolic coated structures. This phenomenon, inducing an arrest of CME, might also be

responsible for a general recycling defect of fundamental compounds of the endosomal pathways.

An alternative mechanism for alteration of endosomal trafficking is that silibinin inhibits fusion between endocytic vesicles and endosomes. Our previous (Wagoner *et al.*, 2011) and present reports clearly show that silibinin is a potent inhibitor of HCVpp/liposome fusion. Rab5 regulates endosome fusion; a common feature of Rabs and AP-2 is their shuttling between cytosol and organelle membranes, where binding is achieved through two geranylgeranyl lipids and recognition of specific phosphoinositides respectively (Kirchhausen, 2002). From our data, lipids may therefore be the common denominator between silymarin-derived molecules (silibinin in particular), HCV and endosomal traffic. Effects of these molecules are evident within minutes of cell, virus or liposomal membrane treatment, presumably reflecting the rate of drug diffusion across or incorporation into membranes. All pure compounds inhibited HCV fusion in doses comparable to the previously reported antiviral IC<sub>50</sub> values (Polyak *et al.*, 2010). Biochemical analyses performed by surface plasmon resonance revealed that both forms of silibinin displayed tropism for lipid membranes, with an apparent affinity in the same micromolar range as the IC<sub>50</sub> for fusion (J.P. Lavergne and E.I. Pécheur, unpubl. data). Along these lines, membranes impregnated by silymarin-derived molecules could become refractory to the recruitment and/or disassembly of machineries required for proper endosomal trafficking and virus entry. This 'lipid' hypothesis is supported by our data on viruses such as VSV and reovirus, and by data from others on alphaviruses (Pohjala *et al.*, 2011), which all enter their target cells partly or exclusively by CME. Silibinin blocked infection by these viruses at similar IC<sub>50</sub> values as those inhibiting HCV entry, fusion and infection (Polyak *et al.*, 2010; Wagoner *et al.*, 2011). Also silibinin-laden membranes could become refractory to fusion, reminiscent of what we described for HCV fusion inhibition by the small molecule arbidol (Teissier *et al.*, 2011).

Our results point to a mode of action where, *in cellulo*, silibinin prevents HCV infection by hindering both viral entry and endosomal trafficking. A clear impact on CME was observed and might be responsible at least in part for the antiviral activity of silibinin. Our findings *in cellulo* that silibinin can prevent infection by distinct viruses strongly suggest that silibinin has a global cellular effect rather than a specific antiviral activity directed against a precise viral function.

Silibinin has been used for decades as a hepatoprotectant and no associated toxicity has been described to date. As such it is unlikely that silibinin, when injected to patients under the Legalon-SIL<sup>®</sup> form, also induces arrest of CME. The molecular mechanisms by which silibinin prevents HCV infection in patients and reinfection of liver graft (Beinhardt *et al.*, 2011) remain elusive. Given the absence of toxicity, it is legitimate to assume that CME is not completely arrested, but that the endocytosis rate is mildly decreased which would alter the very early steps of HCV entry with subsequent perturbations at the fusion stage. Slight perturbations in the timing of occurrence of this subtly controlled phenomenon might address HCV particles to a degradation route instead of a productive path of infection. Silibinin has also been shown to

impact on later stages of HCV infection such as HCV replication, both *in cellulo* and in clinics (Polyak *et al.*, 2010; 2013; Wagoner *et al.*, 2011; Esser-Nobis *et al.*, 2013). Silibinin failed to inhibit replication of various HCV genotypes as a consequence of a mutation in the non-structural protein NS4B (Esser-Nobis *et al.*, 2013). Therefore the exact mode of action of silibinin in patients has to be further characterized, since the immunomodulatory effects of silibinin (inhibition of T cell proliferation, suppression of inflammation) might also explain its antiviral activity (Wagoner *et al.*, 2011; McClure *et al.*, 2012).

Currently approved anti-HCV therapies are based on pegylated-IFN, ribavirin and specific inhibitors of HCV enzymes. This multidrug regimen has proven effective (Farnik and Zeuzem, 2012); however, although it reduces viral load in infected patients, it does not prevent virus propagation as it does not target viral entry steps. Adding to this regimen an antiviral compound like silibinin that targets early steps of HCV life cycle would help improve the efficiency of the therapy.

## **Experimental procedures**

### **Cells and viruses**

PHH were isolated from encapsulated liver resections of two different donors (357 and 366) (Pichard *et al.*, 2006). PHH were kept for three days in Lanford medium at 37°C in a humidified 5% CO<sub>2</sub> atmosphere. Cells were pretreated with CPZ (20 µg ml<sup>-1</sup>, 90 min) and infected with 25 µl of serum HCV gt 1b or 3a (viral loads respectively 2.1 × 10<sup>7</sup> and 7.0 × 10<sup>6</sup> RNA copies ml<sup>-1</sup>). After 16 h at 37°C, inoculum was removed, monolayers washed with William's E medium and fresh Lanford medium was added. Cells were harvested 72 h post-infection. Total RNA was isolated using a guanidinium isothiocyanate solution (RNable, Eurobio), and assayed by Nanodrop™ at 260 nm. Intracellular levels of positive strand HCV RNA were quantified by a RT-qPCR technique using the SuperScript III Platinum One-Step quantitative RT-PCR system (Invitrogen) and a LightCycler®480 Real-Time PCR System. Huh7.5 and BSC1 cells were grown as described (Polyak *et al.*, 2010; Boulant *et al.*, 2011). JFH-1 stock preparation and titration was performed as in (Wakita *et al.*, 2005). Mammalian reovirus virions strains T1L, derived from stocks obtained from B.N. Fields, were grown and purified as described (Furlong *et al.*, 1988). Virions were titrated by plaque assay (Middleton *et al.*, 2002).

### **Cell viability assays**

PHH from the liver donor FT383 were seeded on a 96-well plate and treated in the conditions used for the infection test. All experiments were performed in triplicates. After 48 h of contact with Legalon-SIL® or SbN, supernatant was removed, 50 µl PBS were added, followed by 50 µl of CellTiter-Glo reagent (Promega luminescent assay). Bioluminescence was measured 10 min later using a Mithras LB940 microplate reader (Berthold Technologies, Thoiry, France). Huh7.5 cell viability in the presence of increasing concentrations of Legalon-SIL® or SbN was assessed using the tetrazolium-derived compound MTS (Cory *et al.*, 1991).

## **Silymarin, silibinin and pure compounds**

They were prepared and used as described (Graf *et al.*, 2007; Polyak *et al.*, 2010; Wagoner *et al.*, 2010). Legalon-SIL<sup>TM</sup> was a kind gift of R.T. Pohl (Madaus GmbH, Cologne, Germany).

## **HCVpp labelling and fusion assays**

Concentrated HCVpp prepared as in (Bartosch *et al.*, 2003; Teissier *et al.*, 2011) were incubated with 2  $\mu$ M R<sub>18</sub> (final) at 4°C for 30 min, as described (Lavillette *et al.*, 2006). After a 16 h centrifugation at 150 000 g on a 20–60% sucrose gradient at 4°C, 0.7 ml fractions were collected, assayed for integrity by TEM observation, for infectivity through luciferase expression (Chapel *et al.*, 2007), for E2 and mouse leukaemia virus GAG by immuno-fluorescence, and for R<sub>18</sub> fluorescence. Only fractions combining all proper readouts were used for live cell imaging, after sucrose removal by a 45 min centrifugation at 150 000 g and resuspension in ice-cold PBS. Fusion between HCVpp and R<sub>18</sub>-labelled liposomes was performed as in Lavillette *et al.* (2006).

## **Transmission electron microscopy**

Huh7.5 cells infected by JFH-1 virus (MOI 3) were prepared for TEM observation after immuno-gold labelling with the anti-E2 antibody AP-33, as described in details in (Maillard *et al.*, 2011). In some experiments, cells were preincubated with the human monoclonal antibody CBH-5 (10  $\mu$ g ml<sup>-1</sup>), targeting HCV E2, before adding JFH-1 virions and further labelling of HCV core.

## **Immunofluorescence microscopy**

Huh7.5 cells (40 000 per well) were seeded onto 13 mm round coverslips 24 h prior to infection. Cells were washed with PBS and culture medium containing 80  $\mu$ M SbN or DMSO was added for 1 h. Cells placed on ice were infected 1 h with JFH-1 HCV (MOI 1). Unbound virus was washed off with PBS, culture medium with or without silibinin added and cells transferred to 37°C. Coverslips were fixed with 2% PFA, 30 min, 60 or 90 min post-temperature shift. HCV was immunostained with a monoclonal mouse anti-core antibody (C7-50, AbCam), and endocytic compartments with anti-clathrin, anti-Rab5, anti-Lamp1 or anti-Rab7 antibodies (Abcam). Coverslips were imaged using Leica Confocal Spectral TCS SP5 AOBS.

Viral infectivity under SbN or Legalon-SIL<sup>®</sup> treatment of Huh7.5 cells was determined by serial dilutions of JFH-1 virions, starting from a MOI of 1. After 72 h in culture, cells were fixed in methanol/acetone, and prepared for immunofluorescence of HCV core using the C7-50 antibody. Fluorescent foci of infection (expressed as FFU ml<sup>-1</sup>; FFU, focus-forming units) were then counted under the microscope, in three separate experiments.

## **Transferrin uptake**

Huh7.5 cells were pretreated at 37°C with 50 or 80  $\mu\text{M}$  SbN for 10 or 25 min in Dulbecco's modified Eagle's medium (DMEM) with 10% FBS. Cells washed with PBS were incubated with Alexa647-labelled Trf (50  $\mu\text{g ml}^{-1}$  final) in supplemented DMEM with or without 50 or 80  $\mu\text{M}$  silibinin for 7 min at 37°C. Cells were washed with ice-cold PBS to remove unbound Trf, and fixed with 4% PFA. Trf uptake quantification was performed by fluorescent confocal microscopy. Cells showing Alexa647-fluorescent Trf localized in the nucleus vicinity were considered positive. Cells revealing little to no labelled Trf in their interior, with labelled Trf located at the plasma membrane were considered negative. At least 50 cells were scored for each condition.

### **Influenza virus and reovirus infection**

MDCK cells were allowed to polarize by seeding on coverslips 2–3 days prior to infection. Cells treated or not with SbN for 30 min were inoculated with influenza viruses 1 h at 37°C, and washed. To evaluate SbN effect on post-entry steps, drug was added to cells 1 h post wash-out.

For reovirus infection, MDCK cells were washed with PBS, and DMEM containing 80  $\mu\text{M}$  SbN or DMSO was added for 20 min at 37°C. Reovirus virions or ISVPs were added to cells at a MOI giving 50% infected cells in mock-treated conditions, for 2 h at 37°C in the absence or presence of increasing SbN doses. Cells were washed with ice-cold PBS and monoclonal anti- $\sigma 1$  5E6 neutralizing antibody was added for 2 h at 4°C (final concentration 1–2  $\mu\text{g ml}^{-1}$ ). After ice-cold PBS washes, fresh complete medium was added to cells for 8–12 h at 37°C. Cells were then fixed with 4% PFA and immunostained using a polyclonal rabbit anti- $\mu\text{NS}$ . The fraction of infected cells was assessed by fluorescent microscopy.

### **VSV infection assay**

BSC1 cells were pretreated with SbN or DMSO (mock). VSV was added to the cells for 30 min. Virions were removed by washing the cells and medium containing SbN was added to SbN-pretreated cells and, as a control both for cell viability and aspecific effect of the drug, medium containing SbN was added to mock-treated cells.

### **Live-cell imaging, data acquisition and image analysis**

BSC1 cells expressing AP-2  $\sigma 2$  subunit fused to eGFP were plated 12–16 h at 37°C prior to imaging. Cells were placed in a perfusion chamber and maintained in phenol red-free DMEM supplemented with 10% FBS and 20 mM Hepes pH 7.4. Medium was replaced by 50 or 80  $\mu\text{M}$  SbN in same medium. At various times post-SbN addition, CCP formation dynamics were monitored by live-cell fluorescent spinning disk confocal microscopy imaging the bottom surface of the cells [in contact with the coverslip (Saffarian *et al.*, 2009)]. Images were captured using Slidebook 5 (Intelligent Imaging 3i). Movies were acquired at a 0.5 Hz frequency using a 50 ms exposure time, 100 frames total. AP-2-coated fluorescent structures were identified and tracked using MATLAB IMAB software (Boulant *et al.*, 2011).

Huh7.5 cells (40 000 per well) were seeded for 24 h on two-well LAB-TEKI chamber and transfected with eGFP-clathrin using JetPrime™ Polyplus-transfection (Ozyme) according to manufacturer. Alternatively Huh7.5 cells were transduced with the CellLight® Early Endosomes-eGFP \*BacMam 2.0\* (Invitrogen). Live-cell imaging was performed 48 or 72 h post transfection/transduction. Cells were washed with phenol red-free DMEM/F-12 (Invitrogen). Medium containing 80 µM SbN or Legalon-SIL® or DMSO was added to cells for 1 h. Cells placed on ice were infected away from light, 1 h with 40 µl of R<sub>18</sub>-labelled purified HCVpp. Unbound virus was washed off with 37°C DMEM/F-12 containing SbN, Legalon-SIL® or DMSO. The plate was placed in the 37°C-thermostated microscope chamber with 5% CO<sub>2</sub>. Virion trafficking was monitored by live-cell fluorescent spinning disk confocal microscopy. Images were acquired by taking sequential RFP/eGFP exposures at 200–400 ms every 800 ms for 15 min or every 30 s for 150 min, using the 7.5.4 Metamorph software (Molecular Devices). Fluorescent clathrin-coated structures, Rab5-positive endosomes and virions were identified using ImageJ (<http://imagej.nih.gov/ij/>). Trajectories were determined using ImageJ plug-in Manual\_Tracking (<http://rsbweb.nih.gov/ij/plugins/track/track.html>).

### **Statistical analyses**

Images of virion trafficking were taken every 30 s for 150 min, on a randomly chosen panel of 25 cells, and two separate experiments were performed. Using image treatment methods, numbers of clathrin-coated or Rab5-positive structures and of virions were counted. Then the number of colocalization events between clathrin or Rab5 structures and HCV was calculated. To estimate the measurement error on this number and HCV, the mean value and standard deviation of these quantities were calculated using counts over a 6 min period. The ratio of colocalization events over HCV was computed to be independent of cell size. The ROOT TEfficiency method based on the Clopper-Pearson confidence limits was used (<http://root.cern.ch/root/html/TEfficiency.html>), since the number of events evaluated was not following a gaussian distribution. Other statistical analyses were performed using the Student's *t*-test.

### **Acknowledgements**

We thank C.M. Rice for Huh7.5 cells, J. Dubuisson for HCVpp plasmids and antibodies, T. Wakita for JFH-1 virus, P. Briolotti for expert technical assistance with PHH cultures, R-T. Pohl for kind gift of Legalon-SIL™, C. Chamot, O. Duc and C. Lionnet for training and help with cell imaging (PLATIM, ENS Lyon), J.J. Blaising (CERN, Geneva) for expertise on statistical analyses, the Centre Technique des Microstructures for TEM imaging (Université Lyon 1), A.H. Patel for AP-33, S. Fong for CBH-5 antibody, and J. Klinghauf for eGFP-clathrin plasmid. E-I.P. is supported by FINOVI foundation and ANRS. S.B. was supported by the Harvard Digestive Disease Consortium Feasibility Award, a GlaxoSmithKline fellowship and the CHS foundation, Germany. S.J.P and N.H.O. are partially supported by NIH grant R01AT006842. J.B. is the recipient of a PhD grant from Cluster Infectiologie Région Rhône Alpes.

## References

- Ahmed-Belkacem, A., Ahnou, N., Barbotte, L., Wychowski, C., Pallier, C., Brillet, R., *et al.* (2010) Silibinin and related compounds are direct inhibitors of hepatitis C virus RNA-dependent RNA polymerase. *Gastroenterology* **138**: 1112–1122.
- Bartosch, B., Dubuisson, J., and Cosset, F.L. (2003) Infectious hepatitis C virus pseudo-particles containing functional E1-E2 envelope protein complexes. *J Exp Med* **197**: 633–642.
- Beinhardt, S., Rasoul-Rockenschaub, S., Scherzer, T.M., and Ferenci, P. (2011) Silibinin monotherapy prevents graft infection after orthotopic liver transplantation in a patient with chronic hepatitis C. *J Hepatol* **54**: 591–592; author reply 592–593.
- Blanchard, E., Belouzard, S., Goueslain, L., Wakita, T., Dubuisson, J., Wychowski, C., and Rouille, Y. (2006) Hepatitis C virus entry depends on clathrin-mediated endocytosis. *J Virol* **80**: 6964–6972.
- Boulant, S., Kural, C., Zeeh, J.C., Ubelmann, F., and Kirchhausen, T. (2011) Actin dynamics counteract membrane tension during clathrin-mediated endocytosis. *Nat Cell Biol* **13**: 1124–1131.
- Boulant, S., Stanifer, M., Kural, C., Cureton, D.K., Massol, R., Nibert, M.L., and Kirchhausen, T. (2013) Similar uptake but different trafficking and escape routes of reovirus virions and ISVPs imaged in polarized MDCK cells. *Mol Biol Cell* **24**: 1196–1207.
- Chandran, K., Farsetta, D.L., and Nibert, M.L. (2002) Strategy for nonenveloped virus entry: a hydrophobic conformer of the reovirus membrane penetration protein micro 1 mediates membrane disruption. *J Virol* **76**: 9920–9933.
- Chapel, C., Garcia, C., Bartosch, B., Roingard, P., Zitzmann, N., Cosset, F.L., *et al.* (2007) Reduction of the infectivity of hepatitis C virus pseudoparticles by incorporation of misfolded glycoproteins induced by glucosidase inhibitors. *J Gen Virol* **88**: 1133–1143.
- Codran, A., Royer, C., Jaeck, D., Bastien-Valle, M., Baumert, T.F., Kieny, M.P., *et al.* (2006) Entry of hepatitis C virus pseudotypes into primary human hepatocytes by clathrin-dependent endocytosis. *J Gen Virol* **87**: 2583–2593.
- Coller, K.E., Berger, K.L., Heaton, N.S., Cooper, J.D., Yoon, R., and Randall, G. (2009) RNA interference and single particle tracking analysis of hepatitis C virus endocytosis. *PLoS Pathog* **5**: e1000702.
- Cory, A.H., Owen, T.C., Barltrop, J.A., and Cory, J.G. (1991) Use of an aqueous soluble tetrazolium/formazan assay for cell growth assays in culture. *Cancer Commun* **3**: 207–212.

- Cureton, D.K., Massol, R.H., Saffarian, S., Kirchhausen, T.L., and Whelan, S.P. (2009) Vesicular stomatitis virus enters cells through vesicles incompletely coated with clathrin that depend upon actin for internalization. *PLoS Pathog* **5**: e1000394.
- Cureton, D.K., Harbison, C.E., Cocucci, E., Parrish, C.R., and Kirchhausen, T. (2012) Limited transferrin receptor clustering allows rapid diffusion of canine parvovirus into clathrin endocytic structures. *J Virol* **86**: 5330–5340.
- Dahari, H., Guedj, J., and Perelson, A.S. (2011) Silibinin mode of action against hepatitis C virus: a controversy yet to be resolved. *Hepatology* **54**: 749.
- Davis-Searles, P.R., Nakanishi, Y., Kim, N.C., Graf, T.N., Oberlies, N.H., Wani, M.C., *et al.* (2005) Milk thistle and prostate cancer: differential effects of pure flavonolignans from *Silybum marianum* on antiproliferative end points in human prostate carcinoma cells. *Cancer Res* **65**: 4448–4457.
- Ehrlich, M., Boll, W., Van Oijen, A., Hariharan, R., Chandran, K., Nibert, M.L., and Kirchhausen, T. (2004) Endocytosis by random initiation and stabilization of clathrin-coated pits. *Cell* **118**: 591–605.
- Esser-Nobis, K., Romero-Brey, I., Ganten, T.M., Gouttenoire, J., *et al.* (2013) Analysis of hepatitis C virus resistance to silibinin *in vitro* and *in vivo* points to a novel mechanism involving nonstructural protein 4B. *Hepatology* **57**: 953–963.
- Farnik, H., and Zeuzem, S. (2012) New antiviral therapies in the management of HCV infection. *Antivir Ther* **17**: 771–783.
- Farquhar, M.J., Hu, K., Harris, H.J., Davis, C., Brimacombe, C.L., Fletcher, S.J., *et al.* (2012) Hepatitis C virus induces CD81 and claudin-1 endocytosis. *J Virol* **86**: 4305–4316.
- Ferenci, P., Scherzer, T.M., Kerschner, H., Rutter, K., Beinhardt, S., Hofer, H., *et al.* (2008) Silibinin is a potent antiviral agent in patients with chronic hepatitis C not responding to pegylated interferon/ribavirin therapy. *Gastroenterology* **135**: 1561–1567.
- Furlong, D.B., Nibert, M.L., and Fields, B.N. (1988) Sigma 1 protein of mammalian reoviruses extends from the surfaces of viral particles. *J Virol* **62**: 246–256.
- Graf, T.N., Wani, M.C., Agarwal, R., Kroll, D.J., and Oberlies, N.H. (2007) Gram-scale purification of flavonolignan diastereoisomers from *Silybum marianum* (Milk Thistle) extract in support of preclinical *in vivo* studies for prostate cancer chemoprevention. *Planta Med* **73**: 1495–1501.
- Haid, S., Pietschmann, T., and Pécheur, E.I. (2009) Low pH-dependent hepatitis C virus membrane fusion depends on E2 integrity, target lipid composition, and density of virus particles. *J Biol Chem* **284**: 17657–17667.

- Hawke, R.L., Schrieber, S.J., Soule, T.A., Wen, Z., Smith, P.C., Reddy, K.R., *et al.* (2010) Silymarin ascending multiple oral dosing phase I study in noncirrhotic patients with chronic hepatitis C. *J Clin Pharmacol* **50**: 434–449.
- Kirchhausen, T. (2002) Clathrin adaptors really adapt. *Cell* **109**: 413–416.
- Lavillette, D., Bartosch, B., Nourrisson, D., Verney, G., Cosset, F.L., Penin, F., and Pécheur, E.I. (2006) Hepatitis C virus glycoproteins mediate low pH-dependent membrane fusion with liposomes. *J Biol Chem* **281**: 3909–3917.
- McClure, J., Lovelace, E.S., Elahi, S., Maurice, N.J., Wagoner, J., Dragavon, J., *et al.* (2012) Silibinin inhibits HIV-1 infection by reducing cellular activation and proliferation. *PLoS ONE* **7**: e41832.
- Maillard, P., Walic, M., Meuleman, P., Roohvand, F., Huby, T., Le Goff, W., *et al.* (2011) Lipoprotein lipase inhibits hepatitis C virus (HCV) infection by blocking virus cell entry. *PLoS ONE* **6**: e26637.
- Martinez, C.G., Guinea, R., Benavente, J., and Carrasco, L. (1996) The entry of reovirus into L cells is dependent on vacuolar proton-ATPase activity. *J Virol* **70**: 576–579.
- Meertens, L., Bertaux, C., and Dragic, T. (2006) Hepatitis C virus entry requires a critical postinternalization step and delivery to early endosomes via clathrin-coated vesicles. *J Virol* **80**: 11571–11578.
- Mercer, J., Schelhaas, M., and Helenius, A. (2010) Virus entry by endocytosis. *Annu Rev Biochem* **79**: 803–833.
- Middleton, J.K., Severson, T.F., Chandran, K., Gillian, A.L., Yin, J., and Nibert, M.L. (2002) Thermostability of reovirus disassembly intermediates (ISVPs) correlates with genetic, biochemical, and thermodynamic properties of major surface protein mu1. *J Virol* **76**: 1051–1061.
- Mukherjee, S., and Sorrell, M.F. (2008) Controversies in liver transplantation for hepatitis C. *Gastroenterology* **134**: 1777–1788.
- Pichard, L., Raulet, E., Fabre, G., Ferrini, J.B., Ourlin, J.C., and Maurel, P. (2006) Human hepatocyte culture. *Methods Mol Biol* **320**: 283–293.
- Pohjala, L., Utt, A., Varjak, M., Lulla, A., Merits, A., Ahola, T., and Tammela, P. (2011) Inhibitors of alphavirus entry and replication identified with a stable Chikungunya replicon cell line and virus-based assays. *PLoS ONE* **6**: e28923.

- Polyak, S.J., Morishima, C., Shuhart, M.C., Wang, C.C., Liu, Y., and Lee, D.Y. (2007) Inhibition of T-cell inflammatory cytokines, hepatocyte NF-kappaB signaling, and HCV infection by standardized Silymarin. *Gastroenterology* **132**: 1925–1936.
- Polyak, S.J., Morishima, C., Lohmann, V., Pal, S., Lee, D.Y., Liu, Y., *et al.* (2010) Identification of hepatoprotective flavonolignans from silymarin. *Proc Natl Acad Sci USA* **107**: 5995–5999.
- Polyak, S.J., Oberlies, N.H., Pécheur, E.I., Ferenci, P., and Pawlotsky, J. (2013) Silymarin for HCV infection. *Antivir Ther* **18**: 141–147.
- Rust, M.J., Lakadamyali, M., Zhang, F., and Zhuang, X. (2004) Assembly of endocytic machinery around individual influenza viruses during viral entry. *Nat Struct Mol Biol* **11**: 567–573.
- Rutter, K., Scherzer, T.M., Beinhardt, S., Kerschner, H., Stattermayer, A.F., Hofer, H., *et al.* (2011) Intravenous silibinin as ‘rescue treatment’ for on-treatment non-responders to pegylated interferon/ribavirin combination therapy. *Antivir Ther* **16**: 1327–1333.
- Saffarian, S., Cocucci, E., and Kirchhausen, T. (2009) Distinct dynamics of endocytic clathrin-coated pits and coated plaques. *PLoS Biol* **7**: e1000191.
- van der Schaar, H.M., Rust, M.J., Chen, C., van der Ende-Metselaar, H., Wilschut, J., Zhuang, X., and Smit, J.M. (2008) Dissecting the cell entry pathway of dengue virus by single-particle tracking in living cells. *PLoS Pathog* **4**: e1000244.
- Schulz, W.L., Haj, A.K., and Schiff, L.A. (2012) Reovirus uses multiple endocytic pathways for cell entry. *J Virol* **86**: 12665–12675.
- Tamayo, C., and Diamond, S. (2007) Review of clinical trials evaluating safety and efficacy of milk thistle (*Silybum marianum* [L.] Gaertn.). *Integr Cancer Ther* **6**: 146–157.
- Teissier, E., Zandomenighi, G., Loquet, A., Lavillette, D., Lavergne, J.P., Montserret, R., *et al.* (2011) Mechanism of inhibition of enveloped virus membrane fusion by the antiviral drug arbidol. *PLoS ONE* **6**: e15874.
- Tscherne, D.M., Jones, C.T., Evans, M.J., Lindenbach, B.D., McKeating, J.A., and Rice, C.M. (2006) Time- and temperature-dependent activation of hepatitis C virus for low-pH-triggered entry. *J Virol* **80**: 1734–1741.
- Wagoner, J., Negash, A., Kane, O.J., Martinez, L.E., Nahmias, Y., Bourne, N., *et al.* (2010) Multiple effects of silymarin on the hepatitis C virus lifecycle. *Hepatology* **51**: 1912–1921.

Wagoner, J., Morishima, C., Graf, T.N., Oberlies, N.H., Teissier, E., Pécheur, E.I., *et al.* (2011) Differential in vitro effects of intravenous versus oral formulations of silibinin on the HCV life cycle and inflammation. *PLoS ONE* **6**: e16464.

Wakita, T., Pietschmann, T., Kato, T., Date, T., Miyamoto, M., Zhao, Z., *et al.* (2005) Production of infectious hepatitis C virus in tissue culture from a cloned viral genome. *Nat Med* **11**: 791–796.

Yim, Y.I., Sun, T., Wu, L.G., Raimondi, A., De Camilli, P., Eisenberg, E., and Greene, L.E. (2010) Endocytosis and clathrin-uncoating defects at synapses of auxilin knockout mice. *Proc Natl Acad Sci USA* **107**: 4412–4417.